Community Composition of Bacteria Isolated from Swiss Banknotes Varies Depending on Collection Environment

Running title: Variable Monetary Microbiome in Switzerland

Authors: Anna M. Bischofberger[1†], Alex R. Hall[1]

Contact information: [1]Institute of Integrative Biology, ETH Zurich, Switzerland

[†]anna.bischofberger@env.ethz.ch

Abstract:

Humans interact constantly with surfaces and associated microbial communities in the environment. The factors shaping the composition of these communities are poorly understood: some proposed explanations emphasize the influence of local habitat conditions (niche-based explanations), while others point to geographic structure and the distance among sampled locations (dispersal-based explanations). However, the relative roles of these different drivers for microbial community assembly on human-associated surfaces are not clear. Here, we used a combination of sampling, sequencing (16S rRNA) and culturing to show that the composition of banknote-associated bacterial communities varies depending on the local collection environment. Using banknotes collected from various locations and types of shops across Switzerland, we found taxonomic diversity dominated by families such as *Pseudomonadaceae* and *Staphylococcaceae*, but with banknote samples from particular types of shops (especially butcher shops) having distinct community structure. By contrast, we found no evidence of geographic structure: similarity of community composition did not decrease with increasing distance among sampled locations. These results show that microbial communities associated with banknotes, one of the most commonly encountered and exchanged human-associated surfaces, can reflect the local environmental conditions (in this case, the type of shop), and the signal for this type of variation was stronger than that for geographic structure among the locations sampled here.

Keywords:

microbiome, banknote, community assembly, 16S rRNA

Introduction

Humans encounter microbial communities constantly and we now know that they contribute, among other things, to food and drink quality (Wareing, 2016; Reese *et al.*, 2020), soil fertility (Fierer, 2017) and human health (Libertucci and Young, 2019). Understanding variation of microbial community structure (relative abundances of different taxa) is therefore an important challenge. As for other organisms and in the wider field of community ecology, the contributions of different drivers of microbial community assembly remain unclear (Chesson, 2000; Ebach, 2015). Selection imposed by local habitat conditions and biotic interactions (niche-based explanations invoking deterministic factors) (Macarthur and Levins, 1967; Diamond, 1975) is expected to result in communities matched to their local environments. Other possible drivers include more stochastic processes, ecological drift or dispersal limitation (Hubbell, 2011), which may result in geographic structuring of communities independent from the effects of local habitat conditions. There is evidence from microbes and other taxa supporting both types of explanation (Finlay, 2002; Fargione *et al.*, 2003; Whitaker *et al.*, 2003a; Horner-Devine *et al.*, 2004; Zhou *et al.*, 2013; Webb), and it is increasingly recognised that multiple drivers are in play (Chase, 2003a; Chase and Myers, 2011; HilleRisLambers *et al.*, 2012). However, we still lack a clear picture of their relative roles (Chase, 2010; Hanson *et al.*, 2012; Stegen *et al.*, 2015; Zhou and Ning, 2017). This problem is especially acute for microbial communities on surfaces that humans interact with in daily life. For example, a recent global study of microbial communities on metro and transit systems identified city-specific community composition linked to local conditions, albeit with a shared core microbiota across locations (Danko *et al.*, 2021). However, it is not yet clear whether such biogeographical structuring is also evident on other human-associated surfaces, or how strongly such microbiomes reflect local habitat conditions (selection) as opposed to other predictors such as geographic distance among sites.

57 One of the most important human-associated surfaces is cash money: few everyday objects
58 are as frequently, widely and actively exchanged among humans as banknotes. Paper-based
59 money has been in use for hundreds of years and is now commonplace around the world.
60 Despite the advent of credit cards and other cashless payment instruments, banknotes and coins
61 are still the most common payment option for purchases at the physical point of sale and for
62 person-to-person payments in the EU and Switzerland (Central Bank, 2020; Gehring *et al.*).
63 The rough surface of most banknotes lends itself well to the attachment of microorganisms
64 (Jalali *et al.*, 2015; Vriesekoop *et al.*, 2016), something first investigated in the late 19th century
65 (Schaarschmidt, 1884). Since then, tools such as metagenomic sequencing have enabled more
66 detailed description of microorganisms on money, including characterization of communities
67 on dollar bills in New York City (Maritz *et al.*, 2017), identification of pathogens and antibiotic
68 resistance genes on Rupees in New Delhi (Jalali *et al.*, 2015), and monitoring survival of
69 influenza viruses on banknotes (Thomas *et al.*, 2008). However, to our knowledge it remains
70 poorly understood whether banknotes collected in different places harbour microbial
71 communities that reflect their local environment, which would indicate a role for selection
72 (Hanson *et al.*, 2012; Zhou and Ning, 2017), and/or show biogeographic structuring (e.g.,
73 increasing dissimilarity with geographic distance).
74 Here, we aimed to quantify variation of the bacterial microbiome associated with banknotes
75 originating from different locations across a country, and to test whether this variation can be
76 explained by geographic distances among locations, or other characteristics of the local
77 sampling environments. We did this by collecting banknotes from each of ten locations in
78 Switzerland (Fig. 1A), visiting five different types of shops in each location. We hypothesized
79 community composition would vary among banknotes collected from different types of shops
80 (if there is an effect of local habitat selection on the monetary microbiome), and/or that
81 banknotes collected from more distant locations would harbour more dissimilar communities

82 (if there is biogeographic structuring in general). We studied the samples isolated from the 50
83 banknotes by (1) 16S rRNA sequencing to determine community composition, including viable
84 and non-viable, culturable and non-culturable bacteria, and (2) plating on chromogenic agar to
85 detect viable, culturable bacteria. Our results show that the composition of bacterial
86 communities isolated from banknotes – determined by both sequencing and by plating – varies
87 depending on the local environment (shop type) in which banknotes are collected. By contrast,
88 we find no evidence for geographic structuring of bacterial community composition across
89 banknotes sampled in Switzerland.
90

91 **Materials and Methods**

92 **Sample Collection**

93 We collected banknotes from ten locations in Switzerland. In choosing locations, we adhered
94 to several criteria: (1) countrywide distribution of sampled locations (Fig. 1A; (2) fewer than
95 10'000 inhabitants per location (because we expected any signal for geographic structuring
96 would be stronger among smaller towns due to their being, in general, less well connected with
97 each other and with other parts of the country (Chase, 2003b)); (3) all of the targeted shop types
98 (bakery, butcher, florist, kiosk/newsagent, and pharmacy) present at each location; (4) no
99 significant commuter traffic between locations (according to (Federal Office of Statistics,
100 2020); again we expected geographic structuring of microbial communities would be stronger
101 among less connected towns). The chosen locations were (Fig. 1A): Biasca (BIA), Brienz BE
102 (BRI), Frick (FRI), Klosters-Serneus (KLO), Langnau am Albis (LAN), Orbe (ORB),
103 Porrentruy (POR), Rorschach (ROR), Stein am Rhein (STE), Visp (VIS). We chose the five
104 shop types in an attempt to represent different environments, products and clientele. More
105 details on locations and shops can be found in Tables S1 and S2, respectivley.

106 On arrival in a location, we collected the banknotes from the different shops as follows:
107 donning sterile gloves before entering the shop; choosing an item for less than CHF 10; paying
108 the item with a CHF 20 banknote; folding the CHF 10 banknote received as change in half
109 twice and collecting it in a sterile Nasco Whirl-Pak® sample bag (product nr. 11701973; Fisher
110 Scientific AG, Reinach, Switzerland); storing the sample bag in a paper envelope. Once we
111 had the five banknotes of a given location, we transported the banknotes back to the laboratory
112 and did the initial processing as described below. All samples were collected by the same
113 person between March 12th and March 26th, 2021. Samples from different locations were
114 collected on different days. One sample (butcher-BIA) was classified as "butcher" even though
115 it came from a supermarket with a served meat counter (both butchers in Biasca (BIA) were
116 closed on collection day); this is discussed further below. We contacted all shop owners via
117 email to inform them about our project and gave them the option to have the banknote collected
118 in their shop removed from the study. No shop owner vetoed inclusion of the banknote
119 collected in their shop in the study.
120
121 **Initial Sample Processing and Plating**
122 We performed initial processing for all banknotes on the day of collection as follows: after
123 removing the banknote from the sample bag and placing it on a sterile surface, we swabbed the
124 front of the banknote (not exposed to the bag surface) along the width from top to bottom
125 (Maritz *et al.*, 2017), using a sterile cotton swab (product nr. 80.628; Sarstedt, Nürnberg,
126 Germany) moistened with phosphate-buffered saline (PBS; product nr. P4417-100TAB;
127 Sigma-Aldrich, Merck KgaA, Germany). Turning the banknote 90 degrees, we repeated the
128 procedure. With the same swab, we swabbed the back of the banknote according to the same
129 protocol. We cut the tip of the swab with sterile cissors and placed it in an 2mL Eppendorf tube
130 filled with 950µL PBS. We repeated the procedure with the other four banknotes, sterilizing

131 the surface between samples. As a negative control, we swabbed the interior of a sample bag
132 and followed the protocol just described. We vortexed all Eppendorf tubes for 5min at the
133 highest amplitude and removed the swab tips with sterile tweezers, squeezing out the remaining
134 liquid.

135 To screen for viable and culturable cells, we plated a 50µL aliquot of each sample on a
136 separate Chromatic™ MH agar plate (product nr. LF-611618; Apteq AG, Cham, Switzerland).
137 Chromatic™ MH agar is a chromogenic agar that allows for the identification of bacteria from
138 environmental and clinical isolates by differential colouring of colonies from different species
139 (manufacturer's instructions and colour guide:
140 http://www.liofilchem.net/login/pd/ifu/11618_IFU.pdf) . We incubated plates at 37°C for 24h
141 and stored the remaining samples at -20°C until further processing as described below. Note
142 that plating on chromogenic agar provides a relatively coarse-grained identification and only
143 for certain taxa, but we employed it here only to test (1) for the presence of viable and culturable
144 (i.e., colony-forming) cells and (2) whether the putative species identities of resulting colonies
145 were consistent with taxa identified by sequence analysis. More details on colony morphology
146 and colour can be found in Table S3.

147

148 **Genetic Analysis**

149 We used the DNeasy® PowerLyzer® PowerSoil® Kit (product nr. 12855-100; Qiagen, Hilden,
150 Germany) to extract bacterial DNA from thawed samples, according to the manufacturer's
151 protocol with slight adaptations. In brief: For each sample, we added 700µL to a PowerBead
152 tube (positive control: 700µL PBS plus *Escherichia coli* colony from agar plate; negative
153 control: from empty sample bag, see above) and centrifuged all PowerBead tubes at 13'000rpm
154 for 10min at 4°C. Discarding the supernatant, we dissolved the cell pellet by adding 750µL
155 PowerBead solution and 60µL Solution C1, and inverting the tubes 10 times. After incubating

156 the tubes at 65°C for 10min followed by incubation at 95°C for 10min, we performed bead
157 beating with a Bead Ruptor 24 (Omni International, Inc, Kennesaw (Georgia), United States
158 of America (USA)) with the following settings: cycle nr = 2, strength = 5.5, time = 45s, interval
159 = 0. After transferring the supernatant to clean 2mL collection tubes, we added 250µL Solution
160 C2, vortexed the tubes for 5s at the highest amplitude and incubated them at 4°C for 5min.
161 After centrifugation at 13'000rpm for 1min at 4°C, we transferred 600µL supernatant into clean
162 2mL collection tubes and added 200µL Solution C3. We vortexed tubes briefly at the highest
163 amplitude and incubated them at 4°C for 5min, followed by centrifugation at 13'000 rpm for
164 1min at 4°C. Avoiding the pellet, we transferred 750µL supernatant into clean 2mL collection
165 tubes, added 1200µL well-mixed Solution C4 and vortexed tubes for 5s at the highest
166 amplitude. We loaded 675µL sample onto MB spin Columns, centrifuged them at 13'000rpm
167 for 1min at 4°C and discarded the flow-through. We repeated this until the entire sample was
168 processed. After adding 500µL Solution C5, we centrifuged samples at 13'000rpm for 1min at
169 4°C and discarded the flow-through, followed by centrifugation at 13'000rpm at 4°C for 30s.
170 We placed the MB Spin Columns into clean 2mL collection tubes and added 70µL Solution
171 C6 to the centre of the filter membrane. Following incubation at 65°C for 5min and
172 centrifugation at 13'000rpm at 4°C for 1min, we discarded the MB Spin Columns and stored
173 samples at -20°C. The 50 samples were processed in three batches (consisting of randomly
174 selected samples) on different days, with a positive and negative control for each batch. After
175 sequencing, we did not detect an effect of extraction batch on either read counts per sample
176 (ANOVA: $F_{2,47} = 2.521$, $p = 0.091$) or community composition (PERMANOVA: $F_{2,41} = 1.711$,
177 $p > 0.1$).
178 We quantified the obtained DNA using the Quant-iT™ dsDNA BR Assay Kit (product nr.
179 Q33130; Thermo Fisher Scientific, Waltham, USA) in the Spark® 10M multimode microplate
180 reader (Tecan Group Ltd, Männedorf, Switzerland). We sequenced at the Genetic Diversity

181 Centre, Zurich, Switzerland, using the MiSeq Reagent kit v3 (600 cycle PE) (Illumina, San
182 Diego, USA) after library preparation with the Nextera XT 96 Index kit v2, Set D (Illumina,
183 San Diego, USA). The sequences of the four sets of primers used during library preparation
184 (limited cycle PCR) are listed in Table S4.
185
186 **Bioinformatic Analysis**
187 If not noted otherwise, raw sequence data were processed with USEARCH
188 (v11.0.667_i86linux64; (Edgar, 2010). After end trimming reads (if needed) and merging them
189 into amplicons (commands: *filter_phix*, *filter_lowc* (threshold 25), *fastx_truncate* (trim R1/R2:
190 25/50), *fastx_syncpairs*, *fastq_mergepairs* (min. overlap: 30; min. identity: 60%; min. merged
191 length: 100; min. merged quality: 8)), we trimmed reads for primers (command: *search_pcr*
192 (amplicon size range 100-600; number of mismatches: 2; coverage: full-length (no end gaps)).
193 We used PRINSEQ-lite 0.20.4 (Schmieder and Edwards, 2011) to check quality and size filter
194 (parameters: size range: 150-550; GC range: 30-70; min. Q mean: 20; number of Ns: 1; low
195 complexity: dust / 30). We clustered operational taxonomic units (OTUs) at 97% using the
196 UPARSE-OTU algorithm (number of OTUs: 2378), and used UNOISE3 algorithm to perform
197 denoising (error-correction) of amplicon sequence variants (zero-radius OTUs, number of
198 ZOTUs 100%: 4464), and to cluster ZOTUs at different identity levels (number of ZOTUs
199 99%: 3148; number of ZOTUs 98%: 2513; number of ZOTUs 97%: 2039) (Edgar, 2016b).
200 OTU annotation was carried out using ZOTUs 100% and the SINTAX algorithm (version
201 11.0.667; (Edgar, 2016a)) with Silva 16S (V128) as reference database (tax filter: 0.75).
202 After removing positive and negative controls and mitochondrial and chloroplast sequences,
203 and before filtering, denoised sequencing data (ZOTUs 100%) consisted of 50 samples with
204 14’900’848 raw reads in total, ranging from four to 6’752’341 raw reads per sample (mean
205 number of raw reads: 266’086.57; median number of raw reads 158’243). We filtered data in

206 two steps: (i) removing samples with low number of raw reads (<1000), resulting in the
207 removal of eight samples from the analysis (florist-KLO, butcher-POR, florist-POR, bakery-
208 STE, florist-STE, bakery-BIA, bakery-VIS, florist-LAN) (ii) removal of ZOTUs present at
209 <0.1% of total sequencing depth (which can reduce the read sum for individual samples; total
210 sequencing depth = 14'398'160). After filtering, we had 42 samples with 10'136'186 filtered
211 reads in total, ranging from 138 filtered reads per sample for butcher-BRI to 6'167'513 filtered
212 reads per sample for florist-BRI (mean number of filtered reads = 241'337.76; median number
213 of filtered reads = 88'192; Fig. S1 and Table S5; numbers according to summarize_phyloseq()
214 function in microbiome package (version 1.16.0, (Lahti and Shetty, 2012))). We had at least
215 three samples per location and at least six samples per shop type.
216 The sequencing data have been deposited in the European Nucleotide Archive under the
217 study accession number PRJEB45390 (https://www.ebi.ac.uk/ena; data will be made
218 accessible upon publication of the study).
219
220 **Statistics**
221 We used denoised sequences (ZOTUs 100%) for all analyses, and conducted all analyses in R
222 (version 4.1.2).
223 To quantify within-sample diversity, we used the alpha() function in the microbiome
224 package (version 1.16.0, (Lahti and Shetty, 2012)) on filtered data to calculate several different
225 diversity indices (Shannon diversity index; Gini-Simpson index; observed richness; Chao1
226 index). The Shannon diversity index *H* takes into account both richness and evenness; the Gini-
227 Simpson index gives the probabilty that two random draws from the same sample (with
228 replacement) are not from the same type (here, the same family); the observed richness counts
229 the number of unique species (ZOTUs 100%) present in the sample; Chao1 index is a non-
230 parametric estimator of species richness that assumes Poisson distribution of the data (Chao,

231 1984; Chao and Bunge, 2002). We used analysis of variance (ANOVA) to test whether within-
232 sample diversity varied among locations or shop types (aov() function in the stats package (R
233 version 4.1.3; (R Core Team, 2021))).

234 Before analysing between-sample diversity and to account for different library sizes (Weiss
235 *et al.*, 2017), we normalized filtered data with a regularized-logarithm (rlog() function in the
236 DESeq2 package (version 1.34.0; (Love *et al.*, 2014))), after comparing the two available
237 transformations offered in DESeq2 package, regularized-logarithm transformation and
238 variance-stabilizing transformation. We chose the regularized-logarithm transformation
239 because it (i) is recommended for smaller datasets and for cases with large ranges of sequencing
240 depths across samples (Love *et al.*, 2014); (ii) it performed better in the meanSdPlot generated.

241 As a first test of whether samples from different locations and shop types differed in terms
242 of bacterial community structure, we used permutational multivariate analysis of variance
243 (PERMANOVA; (Anderson, 2001; Zapala and Schork, 2006)) with the adonis2() function in
244 the vegan package (version 2.5-7; (Oksanen *et al.*, 2020)), with filtered-and-normalized data
245 and using Bray-Curtis dissimilarity (vegdist() function) to measure differences among sampled
246 communities. Next, to visualise any clustering among samples in terms of community
247 composition, we performed ordination of filtered-and-normalized data with the ordinate()
248 function in the phyloseq package (version 1.38.0; (McMurdie and Holmes, 2013)), with non-
249 parametric multidmensional scaling (*method* = "NMDS") and Bray-Curtis dissimilarity
250 (*distance* = "bray") as input parameters. We used NMDS as the ordination method because we
251 obtained a stress value of 0.11 for our data with NMDS ordination; stress values <0.2 generally
252 indicate good fit (Clarke, 1993). We visualised ordination results (Fig. 3) with the
253 plot_ordination() function in the phyloseq package (version 1.38.0; (McMurdie and Holmes,
254 2013)). To further characterise beta diversity, we used a heatmap (plot_heatmap() function in
255 phyloseq package version 1.38.0 (McMurdie and Holmes, 2013), relying on (Rajaram and

256 Oono, 2010), with rlog-transformed read data, *method* = "NMDS" and *distance* = "bray";
257 Figure S4) and hierarchical clustering (calculated with hclust() function in the dendextend
258 package version 1.15.2 (Galili, 2015), with a distance matrix based on rlog-transformed read
259 data and Bray-Curtis dissimilarity index and "ward.D2" as method; Figure S5).

260 We used a third type of analysis as an additional test for geographic structuring of microbial
261 community composition, by conducting a Mantel test. This allowed us to account explicitly for
262 the physical distance between individual sampling locations (shops), rather than testing for
263 average differences among locations (as above in PERMANOVA). We did this using the
264 mantel.test() function in the ape package (version 5.5; (Paradis and Schliep, 2019)), with the
265 vegdist() function in the vegan package (version 2.5-7; (Oksanen *et al.*, 2020)) for Bray-Curtis
266 dissimilarity of filtered-and-normalized data. We used the geodist() function in the geodist
267 package (version 0.0.7; (Padgham and Sumner, 2021)) to calculate geographical distance (in
268 metres) between individual sampling locations. We used the same functions when repeating
269 the analysis for sample sets from individual shop types; here and elsewhere, we accounted for
270 multiple testing using the Holm–Bonferroni method (sequential Bonferroni).

271 The core microbiome is defined as the species present above a certain threshold and shared
272 among a set of samples (Salonen *et al.*, 2012; Shade and Handelsman, 2012). We determined
273 the core microbiome, based on ZOTUs 100%, for each shop type as follows: Using filtered-
274 and-normalized relative abundance data (transform() function in the microbiome package
275 (version 1.16.0; "compositional" as input for *transform* argument) and subsetting data by shop
276 type, we applied the core_members() function in the microbiome package (version 1.16.0;
277 (Lahti and Shetty, 2012); *detection* = 0.001 and *prevalence* = 0.5) to filter out core ZOTUs for
278 each shop type. Then, as a fourth analysis of how microbiome structure varies among shop
279 types/locations, we drew a Venn diagram with the venn() function in the eulerr package
280 (version 6.1.0) and determined ZOTU identity with the format_to_besthit() function in the

281 microbiomeutilities package (version 1.00.16; (Lahti *et al.*, 2017)), followed by identification
282 of core ZOTUs with reduce() and intersect() functions (base package, R version 4.1.2; (R Core
283 Team, 2021)). We defined *shared core ZOTUs* as core ZOTUs that appeared in more than one
284 subset (e.g. three shared core ZOTUs in the butcher and in the pharmacy subset, Fig. S2); we
285 defined *unique core ZOTUs* as core ZOTUs that appear in only one subset (e.g. 13 unique core
286 ZOTUs in butcher subset, Fig. S2).

287 To test for an association between the abundance of viable-and-culturable bacteria
288 (presence/absence of colonies and number of colonies per plate, after plating samples on
289 chromatic agar) and shop type and location we conducted hurdle regression for count data via
290 maximum likelihood (hurdle() function in pscl package (version 1.5.5; (Jackman, 2020)), with
291 formula *number.colonies ~ location* or *number.colonies ~ shop.type* and negative binomial
292 regression (with log link) as count model). As our data contained several samples with zero
293 viable cells we adjusted the count table with a dummy variable (dummy species present at
294 count 1 in all samples; (Clarke *et al.*, 2006) to perform further analysis, being aware that we
295 cannot be sure that all empty samples had zero viable cells for the same reason. We used the
296 adjusted count table to perform PERMANOVA as described above.

297 The map of Switzerland with locations (Fig. 1A) was made with the mun.plot() function in
298 RSwissMaps package (version 0.1.0.1; (Zumbach, 2019)) with the following arguments (where
299 relevant): *bfs_id* = dt$bfs_nr, *year* = 2016, *boundaries* = "c". Other packages and functions
300 used in data processing and drawing figures: cowplot (version 1.1.1; (Wilke, 2020)); dplyr
301 (version 1.0.7; (Wickham *et al.*, 2021)); ggplot2 (version 3.3.5; (Wickham, 2009)); ggpubr
302 (version 0.4.0; (Kassambara, 2020)); microbial (version 0.0.20; (Guo and Gao, 2021)); ochRe
303 (version 1.0.0; (Allan *et al.*, 2021)); phyloseq.extended (version 0.1.1.6; (Mahendra, 2019));
304 phylosmith (version 1.0.6; (Smith, 2021)); ranacapa (version 0.1.0; (Kandlikar, 2021)); yarrr

305 (version 0.1.5; (Phillips, 2017)); VennDiagram (version 1.7.0; (Chen, 2021)); vsn (version
306 3.62.0; (Huber *et al.*, 2002)).
307
308 **Results**
309 **Communities Isolated from Banknotes Include *Pseudomonadaceae* and**
310 ***Staphylococcaceae* in All Samples**
311 After filtering the raw data in two steps (see *Methods*), we analysed 42 samples (from originally
312 50 samples) with variable numbers of reads per sample (Fig. S1 and Table S5). We detected
313 some families of bacteria (Fig. 1B) in every banknote sample: *Pseudomonadaceae* and
314 *Staphylococcaceae* were present in all samples (42/42, 100%; Table S6). These are both
315 diverse families that include species closely associated with humans, e.g. as part of the human
316 skin, respiratory tract or gut microbiome (Cogen *et al.*, 2008; Fierer *et al.*, 2008; Murphy and
317 Parameswaran, 2009; Kim *et al.*, 2013; Fourquin-Gomez *et al.*, 2014; Robert-Pillot *et al.*, 2014;
318 Rock and Donnenberg, 2014; Delanghe *et al.*, 2021; Skowron *et al.*, 2021), but have also been
319 isolated from animal hosts and soil and aquatic environments (Cousin, 1999; Madhaiyan *et al.*,
320 2020). Other families were detected in significant abundance, but only in subsets of samples,
321 such as *Vibrionaceae* and *Lactobacillaceae* (in 21 and 30 samples out of 42 respectively). If
322 we plot the same data at the genus level, this supports the same conclusions (Fig. S3, Table
323 S7): the most abundant genera (*Pseudomonas* and *Staphylococcus*) belonged to the top families
324 (*Pseudomonadaceae* and *Staphylococcaceae*) and were present in all samples; *Photobacterium*
325 (family *Vibrionaceae*) was present in 21 samples. Note despite this broad agreement, the top
326 12 genera (Fig. S3) did not correspond exactly to the top 12 families (Fig. 1B), because some
327 families were represented by multiple genera. For example, the family *Micrococcaceae* is
328 represented by three genera in Fig. S3 (*Kocuria, Micrococcus, Rothia*), and consequently the

329 genera corresponding to *Lactobacillaceae* and *Brevibacteriaceae* (*Lactobacillus* and
330 *Brevibacterium*) are not shown, even though they were the 13th and 14th most abundant.
331 The same taxa that we identified as being relatively abundant above resurfaced when we
332 calculated the core microbiome for each shop type (taxa found in >50% of samples per shop
333 type at abundance >0.1%). We identified seven dominant core ZOTUs (Dawson *et al.*, 2017;
334 Cruaud *et al.*, 2020) shared between all shop types, attributed to the genera: *Corynebacterium*,
335 *Propionibacterium*, *Pseudomonas*, *Streptococcus* (n = 2) and *Staphylococcus* (n = 2) (Fig. S2;
336 detection threshold = 0.001, prevalence threshold = 0.5; Table S8). Thus, our sequence data
337 revealed that a small set of ZOTUs was shared among microbial communities associated with
338 Swiss banknotes from different shop types, but those communities were diverse and the relative
339 abundances of individual taxa varied among samples.
340 Within-sample diversity estimated by Shannon diversity index (Fig. 2) did not vary
341 significantly with either geographic location or shop type (ANOVA: effect of shop type – $F_{4,37}$
342 = 0.844, p = 0.506; effect of location – $F_{9,32}$ = 1.013, p = 0.45). We obtained the same
343 qualitative result with an alternative diversity index (Gini-Simpson index), and the two
344 diversity indices were highly correlated with each other (linear regression Gini-Simpson ~
345 Shannon: adjusted R^2 = 0.851). Similarly, within-sample species richness (taken as observed
346 richness (Fig. 2B) or Chao1 index) did not vary significantly among locations or shop types
347 (ANOVA observed richness: effect of shop type – $F_{4,37}$ = 0.326, p = 0.859; effect of location –
348 $F_{9,32}$ = 0.801, p = 0.618; ANOVA Chao1: effect of shop type – $F_{4,37}$ = 0.243, p = 0.912; effect
349 of location – $F_{9,32}$ = 1.041, p = 0.43) and was correlated with Shannon diversity (adjusted R^2
350 = 0.629 for observed richness and R^2 = 0.478 for Chao1). Thus, none of the tested within-
351 sample diversity measures varied significantly among shop types or geographic locations.
352
353

354 **Community Composition Was Specific to Shop Type, but Not Location**

355 Bacterial community composition was more similar among banknotes collected from the same
356 shop type than from different shop types (PERMANOVA: effect of shop type – $F_{4,41} = 1.321$,
357 $p = 0.03$). Visualising the similarities/differences among samples by ordination analysis (non-
358 metric multidimensional scaling NMDS) further supported variation of community
359 composition among shop types (Fig. 3). In particular, several samples from butcher shops
360 clustered together in the top-right corner of the ordination plot (Fig. 3). Note one sample
361 classified as "butcher" but separate from this cluster (butcher-BIA) was collected from a
362 supermarket with a served meat counter but separate cash desk (see *Methods*). Consistent with
363 the variation among shop types being primarily driven by the distinctiveness of butcher shop
364 samples, if we excluded butcher samples from the analysis we no longer found significant
365 variation among shop types (PERMANOVA: effect of shop type, excluding butcher samples
366 – $F_{3,32} = 0.949$, $p = 0.584$); this was not the case when re-running the analysis excluding sample
367 sets from all other shop types, except for florist samples which resulted in marginal non-
368 significance (PERMANOVA: effect of shop type, without florist samples – $F_{3,32} = 1.287$, $p =$
369 0.056). Visualising the clustering of samples using a heatmap (Fig. S4) and hierarchical
370 clustering (Fig. S5) supported a similar pattern, with several butcher samples clustering
371 together.

372 Looking at the ZOTUs making up the core microbiome for each shop type again supported
373 butcher samples as being distinctive: the set of banknotes from butchers (n = 9) had the greatest
374 number of core ZOTUs, both in total and unique to a single shop type (31 core ZOTUs in total,
375 13 unique core ZOTUs; Fig. S2). The 13 core ZOTUs unique to butchers belonged to the
376 following genera: *Photobacterium* (n = 3; family *Vibrionaceae*), *Streptococcus* (n = 2; family
377 *Streptococcaceae*), *Brochothrix* (n = 1; family *Listeriaceae*), *Corynebacterium* (n = 1; family
378 *Corynebacteriaceae*), *Kocuria* (n = 1; family *Micrococcaceae*), *Lactobacillus* (n = 1; family

379 *Lactobacillaceae*), *Lactococcus* (n = 1; family *Staphylococcaceae*), *Novosphingobium* (n = 1;
380 family *Sphingomonadaaceae*), *Staphylococcus* (n = 1; family *Staphylococcaceae*), *Veillonella*
381 (n = 1; family *Veillonellaceae*). This is consistent with our family-level analysis (Fig. 1), where
382 some of the families to which these butcher-associated genera belong were over-represented
383 among butcher samples (e.g., *Vibrionaceae*, *Lactobacillaceae*).

384 A comparison between core ZOTUs unique to butcher samples and NMDS scores (Fig. 3;
385 Table S9) provides further information about the taxa that drive the among-shop-type variation:
386 the *Veillonella* core ZOTU and one *Streptococcus* core ZOTU unique to butchers were among
387 the ten ZOTUs with the highest positive scores for NMDS1; the *Lactococcus* and three
388 *Photobacterium* core ZOTUs unique to butchers were among the ten ZOTUs with the highest
389 positive scores for NMDS2 (again consistent with families *Vibrionaceae* and *Lactobacillaceae*
390 being abundant and over-represented in butcher samples in Fig. 1). Taxa with relatively large
391 negative scores for NMDS1 (Table S9) were mostly those with low abundance (and therefore
392 not represented in Fig. 1B), although a *Pseudmonas* representative was among the 20 ZOTUs
393 with the highest squared-and-rooted scores for NMDS1 (Table S9). The samples at the left of
394 Fig. 3 are therefore poor in a combination of various taxa, but their similar position along this
395 axis was not explained by either shop type or location (the six points include samples from all
396 shop types and four locations).

397 We found no evidence that samples collected in different locations (towns) harboured
398 different bacterial microbiomes (PERMANOVA: effect of location – $F_{9,41} = 1.173$, $p = 0.067$;
399 Fig. 3). In a second test for geographic structuring of the sampled communities (Mantel test),
400 we quantified the association between pairwise similarity among samples in terms of
401 community composition and the geographic distances between sampling locations. This
402 revealed no significant association between the two distance measures, neither in the full
403 dataset (n = 42; Mantel test – z = 39’978’433, $p = 0.751$), nor when performed separately for

404 each shop type (Mantel test, five tests total with p-values corrected for multiple testing – p_{bakery}
405 = 1, $p_{butcher}$ = 1; $p_{florist}$ = 0.315; p_{kiosk} = 1; $p_{pharmacy}$ = 1). There was no association between
406 number of reads and location (ANOVA: effect of location – $F_{9,40} = 0.836$, $p > 0.5$). Thus,
407 unlike for the variation among shop types observed above, we found no evidence that the
408 differences in bacterial community composition among samples increased with geographic
409 distance.

410 The observed variation in community composition among shop types was not explained by
411 variable numbers of reads among samples from different shop types (Fig. S1; effect of shop
412 type in ANOVA – $F_{4,45} = 0.792$, $p > 0.5$). Consistent with this, when we exclude the sample
413 butcher-BRI, which had a very low read number (Fig. S1), our qualitative conclusions remain
414 unchanged (PERMANOVA minus butcher-BRI: effect of shop type – $F_{4,40} = 1.312$, $p = 0.034$;
415 effect of location – $F_{9,40} = 1.054$, $p = 0.277$; Mantel test comparing geographic distance and
416 community composition, minus butcher-BRI: n = 41, z = 38'407'749, $p = 0.691$).

417

418 **Cultivation of Samples on Agar Supports Conclusions Drawn from Sequencing Data**

419 When we plated aliquots of samples on Chromatic™ MH agar plates, we detected a total of
420 157 viable colonies across 24 of 50 plates (48%). The number of colonies per plate varied
421 among samples (Fig. 4), and was highest on average for butcher samples (count model in hurdle
422 regression model for shop type: butcher: $z = 3.44$, $p < 0.001$; all other shop types: $p > 0.05$;
423 Fig. 4). There was no significant variation of the number of colonies per plate among
424 geographic locations (count model in hurdle regression model for location: $p > 0.05$ for all
425 locations). Several plates produced no colonies, but presence/absence of viable colonies was
426 not predicted by either shop type or location (zero hurdle model in hurdle regression model for
427 shop type and for location: $p > 0.05$ for all shop types and all locations).

428 The identity of colonies (as determined by colony morphology and colour on Chromatic™
429 MH agar plates, see *Methods*) corresponded to key taxa identified by sequencing: *E. coli* =
430 *Enterobacteriaceae*; *Staphylococcus aureus* = *Staphlyococcaceae*; *Pseudomonas spp* =
431 *Pseudomonadaceae*; *Klebsiella spp.*, *Enterobacter spp.*, *Serratia spp.* = *Enterobacteriaceae*
432 (Fig. 1B Fig. 4). The exception to this trend was *Enterococcus faecalis* (3/157 colonies or 2%),
433 which belongs to the *Enterococcaceae* family. This was not among the most abundant families
434 in our sequence data (Fig. 1B), and we only found ZOTUs categorized as *Enterococcaceae*
435 prior to filtering the data, indicating it was present but at lower abundances than suggested by
436 colony formation data. For most of the other key taxa identified by sequence data that we did
437 not find on agar plates, prior information about these taxa suggests the growth conditions
438 (Chromatic™ MH agar; 37°C; 24h aerobic incubation) are not conducive to colony formation.
439 For example, *Corynebacteriaceae, Lactobacillaceae*, (environmental) *Moraxellaceae*, and
440 *Vibrionaceae* have growth optima <37°C (De Angelis and Gobbetti, 2011; Vinet and
441 Zhedanov, 2011; Lonvaud-Funel, 2014; Tauch and Sandbote, 2014; Baron *et al.*, 2020). In
442 addition, several of the key taxa (e.g. *Brevibacteriaceae, Corynebacteriaceae*
443 *Halomonadaceae*, *Lactobacillaceae*, *Moraxellaceae*, *Vibrionaceae)* may have required
444 incubation times >24h (Vinet and Zhedanov, 2011; Argandoña *et al.*, 2012a; Forquin and
445 Weimer, 2014; Tauch and Sandbote, 2014; De Angelis and Gobbetti, 2016; Baron *et al.*, 2020),
446 or different media composition such as higher salt or nutrient content (*Halomonadaceae* and
447 *Corynebacteriaceae*, respectively, (Argandoña *et al.*, 2012b; Tauch and Sandbote, 2014)).
448 Therefore, the absence of these taxa from our cultured samples is probably because they do not
449 grow well in these conditions, and does not necessarily contradict our finding them in the
450 sequence data.
451 As above for our community-level sequence data, the relative abundances of different taxa
452 inferred from colony counts on chromatic agar varied among different shop types

453 (PERMANOVA with zero-adjusted Bray-Curtis dissimilarity (Clarke *et al.*, 2006): effect of
454 shop type – $F_{4,49} = 2.507$, $p = 0.003$) but not geographic locations (effect of location – $F_{9,41} =$
455 0.080, $p = 0.701$). Thus, banknotes yielded viable colonies and taxonomic identification on
456 chromatic agar, albeit relatively coarse-grained compared to our sequence data, supporting
457 similar conclusions (both in terms of which taxa were present and variation of community
458 composition with collection environment but not geographic location).
459

460 **DISCUSSION**

461 We found that Swiss banknotes taken directly from circulation harbour a variety of bacterial
462 DNA, with the key taxa (Fig. 1B) including families found before in humans and human-
463 associated environments, e.g. the human skin, gut or respiratory tract microbiome, or human
464 food production (Cogen *et al.*, 2008; Fierer *et al.*, 2008; Murphy and Parameswaran, 2009;
465 Oren, 2011; Fourquin-Gomez *et al.*, 2014; Delanghe *et al.*, 2021; Skowron *et al.*, 2021). The
466 evidence from our data set that community composition varied depending on the shop type in
467 which each banknote was collected is surprising: this suggests money has a microbiome
468 reflecting its local environment, even though we assume banknotes are only transiently
469 exposed to each habitat/shop type. By extension, we expect individual banknotes to have a
470 dynamic microbiome that changes during their "lifecycle" as they pass from one habitat to
471 another. By contrast, we found no evidence for geographic structuring, unlike some previous
472 studies with microbes in other contexts (Whitaker *et al.*, 2003b; Horner-Devine *et al.*, 2004),
473 but consistent with other observations of relatively weak biogeographic structuring in microbes
474 (Hillebrand *et al.*, 2001; Finlay, 2002; Zhou *et al.*, 2008). Our plating results corresponded well
475 with conclusions from sequencing, indicating that at least some taxa are present as viable,
476 culturable cells. Together these observations suggest, on the scale investigated here,
477 deterministic assembly processes (e.g., selection imposed by habitat heterogeneity) are more

478 important drivers of banknote-associated bacterial community composition than other
479 processes associated with geographic distance among sites, such as dispersal limitation (Chase,
480 2010).

481 The taxa we identified as being relatively more abundant on banknotes collected from
482 butcher shops (*Brevibacteriaceae*, *Halomonadaceae*, *Lactobacillaceae*, *Vibrionaceae*) are
483 known to include bacteria previously identified in "meaty" contexts. *Halomonadaceae* and
484 *Brevibacteriaceae* have previously been found in high-salinity environments and salty foods
485 such as poultry skin or Chinese pork cured with salt (Oren, 2011; Fourquin-Gomez *et al.*,
486 2014). *Brevibacteriaceae* and *Vibrionaceae* (including the genera within these families, such
487 as *Photobacterium*, which we detected at high abundance in some butcher samples) are
488 frequently found in samples from butchers, slaughterhouses, abattoirs (Sierra *et al.*, 1995;
489 Pennacchia *et al.*, 2011; Połka *et al.*, 2015; Nieminen *et al.*, 2016; Fuertes-Perez *et al.*, 2019;
490 Dourou *et al.*, 2021). Representatives of the *Lactobacillaceae* family are key species used as
491 starter cultures in production of, and have been isolated from, cured and fermented meat
492 (Deibel *et al.*, 1961; Samelis *et al.*, 1994; Cocolin *et al.*, 2011). This finding – that some
493 "meaty" taxa are overrepresented in butcher samples – supports the link between collection
494 environment and microbiome composition. However, it is important to note that members of
495 the same families have also been isolated from a wide range of other environments including
496 humans, plants, animals and foods (Walter, 2008; Oren, 2011; Felis and Pot, 2014; Forquin
497 and Weimer, 2014; Franz *et al.*, 2014; Leisner and Pot, 2014; Pot *et al.*, 2014; Takemura *et al.*,
498 2014)(Oren, 2011) . Therefore, while our results are consistent with past work finding these
499 taxa in "meaty" environments, they can also occur elsewhere. It is interesting in this context
500 that the sample butcher-BIA – classified as "butcher" but in fact originating from a supermarket
501 till due to the respective location's two butchers being closed on collection day – was relatively

502 impoverished for the taxa linked above to the other butcher samples (butcher-BIA: 0.45%
503 *Brevibacteriaceae*, 0.00% *Halomonadaceae*, 0.07% *Lactobacillaceae*, 0.00% *Vibrionaceae*).
504 At a broader level, the taxa we identified across all shop types are in line with previous
505 research into monetary microbiomes. For example, in a metagenomic analysis of dollar bills
506 from New York City (Maritz *et al.*, 2017) found representatives of several of the families that
507 were dominant in our dataset (including *Staphylococcaceae*, *Micrococcaceae*,
508 *Streptococcaceae*, *Corynebacteriaceae*, and *Moraxellaceae*). Similarly, an analysis of Chinese
509 RMB banknotes and US dollar bills (Lin *et al.*, 2021) revealed the most abundant taxa on the
510 family level were *Moraxellaceae*, *Pseudomonadaceae* and *Enterobacteriaceae* (all abundant
511 in our data set). Other studies of monetary microbiomes identified similarly overlapping sets
512 of taxa, including analysis of Indian Rupee banknotes (*Actinobacteria*, *Bacteriodetes*,
513 *Firmicutes*, and *Proteobacteria*; no lower-taxa resolution available) (Jalali *et al.*, 2015),
514 banknotes from Hong Kong (*Moraxellaceae*, *Micrococcaceae*, *Enterobacteriaceae,*
515 *Vibrionaceae*, *Corynebacteriaceae*, *Pseudomonadaceae*, among others) (Heshiki *et al.*, 2017)
516 and from Brazil (*Enterobacteriaceae*, *Staphylococcaceae*, *Lactobacillaceae*, *Moraxellaceae*,
517 and *Corynebacteriaceae*, among others) (da Fonseca *et al.*, 2015). Our results go beyond past
518 work on monetary microbiomes by showing that the relative abundances of different taxa
519 (families and ZOTUs) vary among collection environments (shop types), but not with
520 geographic distance within a European country.
521 A key implication of our results is that even temporary exposure of banknotes to certain
522 environments is reflected by the community composition of colonizing bacteria. This is
523 surprising because we assume the residence time of individual banknotes in a given shop is
524 short (hours, days or weeks). It also suggests high variability in temporal beta diversity in the
525 monetary microbiome. We found several taxa (ZOTUs) that were unique to particular shop
526 types, and at the family level it was also visible that some taxa were overrepresented in butcher

527 samples. Despite this, analogous to the core microbiome (Danko *et al.*, 2021) found in urban
528 mass transit systems, we found something akin to a core microbiome across our samples in that
529 two families (*Pseudomonadaceae, Staphylococcaceae*) were present in every sample.

530 Another important implication of our results is that many of the key taxa of the monetary
531 microbiome in Switzerland are also present as viable cells (culturable on agar). This raises an
532 interesting question about colonization dynamics in the monetary microbiome. If viable
533 microbes are present on banknotes, are they growing and interacting on the banknote itself?
534 We can speculate the rough surface of most banknotes not only allows attachment of bacteria,
535 but also human skin cells, secretions and remnants of food or products during handling.
536 Potentially, this could support bacterial growth after colonization. If the local
537 microenvironment influences the relative growth/death rates of different taxa, this could even
538 shape community composition and contribute to habitat-specific community composition as
539 we observed here. Alternatively, community composition may be determined primarily at the
540 colonization step, with different shop types harbouring different microbiomes in general (due
541 to local habitat selection), which are "sampled" by banknotes passing through the shop. One
542 avenue for future work aiming to tease apart these different potential drivers of the monetary
543 microbiome would be to experimentally colonize banknotes and track community abundance
544 and composition over time (longitudinal sampling of individual banknotes).

545 We emphasize strongly that our results do not address or make any predictions regarding
546 food hygiene or potential health hazards posed to humans. We were solely interested in the
547 microbial community composition on banknotes and how this relates to the sampling
548 environment. Finding distinct microbiomes in different shop types does not necessarily
549 translate to variable infection risk or indicate variable hygiene standards, only that the local
550 monetary microbiome reflects the local commercial environment. It is, for example, not
551 possible for us to infer how long the sampled bacteria have been present on the banknotes. One

552 limitation of our study is that the SARS-CoV2 pandemic has led to changes in customers'
553 payment behaviour (Kraenzlin *et al.*, 2020). This might influence the transfer of microbiota to
554 banknotes, because of increased hygienic awareness in customers and shop staff. For example,
555 we observed in one case a banknote being disinfected by shop staff (the sample extracted from
556 the banknote from this shop was removed in the initial filtering step due to low read counts,
557 see *Methods*). However if anything we would expect any effect of pandemic-related hygiene
558 measures to make our conclusions conservative: when hygiene standards are less stringent we
559 might expect even more exchange of microbiota between the local environment and banknotes.
560 In addition, further work would be needed to discover how the variation between banknotes
561 from different shop types arises, for example, whether it is correlated with the skin microbiome
562 of shop staff or other surfaces in the shops. Another limitation of our study is the spatial scale
563 and number of shop types. While our study design revealed significant variation among shop
564 types, the lack of geographic structure across Switzerland may differ from that across larger
565 spatial scales or across different currency types.

566 In summary, we found that the bacterial communities associated with Swiss banknotes can
567 vary depending on the environment in which the banknotes were collected and that, by contrast,
568 geographic distance between sampled locations does not predict variation of the associated
569 microbial communities. Our results also show that the most abundant taxa are not only present
570 in the form of cell debris and genetic material, but as viable cells that can form colonies during
571 in vitro cultivation. This raises the question of banknotes potentially being involved in
572 transmission of bacteria between people and the environment, and/or of genes, such as
573 antibiotic resistance genes, among bacteria co-occurring on the same banknotes. Therefore, a
574 key avenue for future work building on the link between microbial community structure on
575 banknotes and the local environment (shop type) identified here is to ask whether this translates
576 to variable infection risk or horizontal gene transfer.

Figures

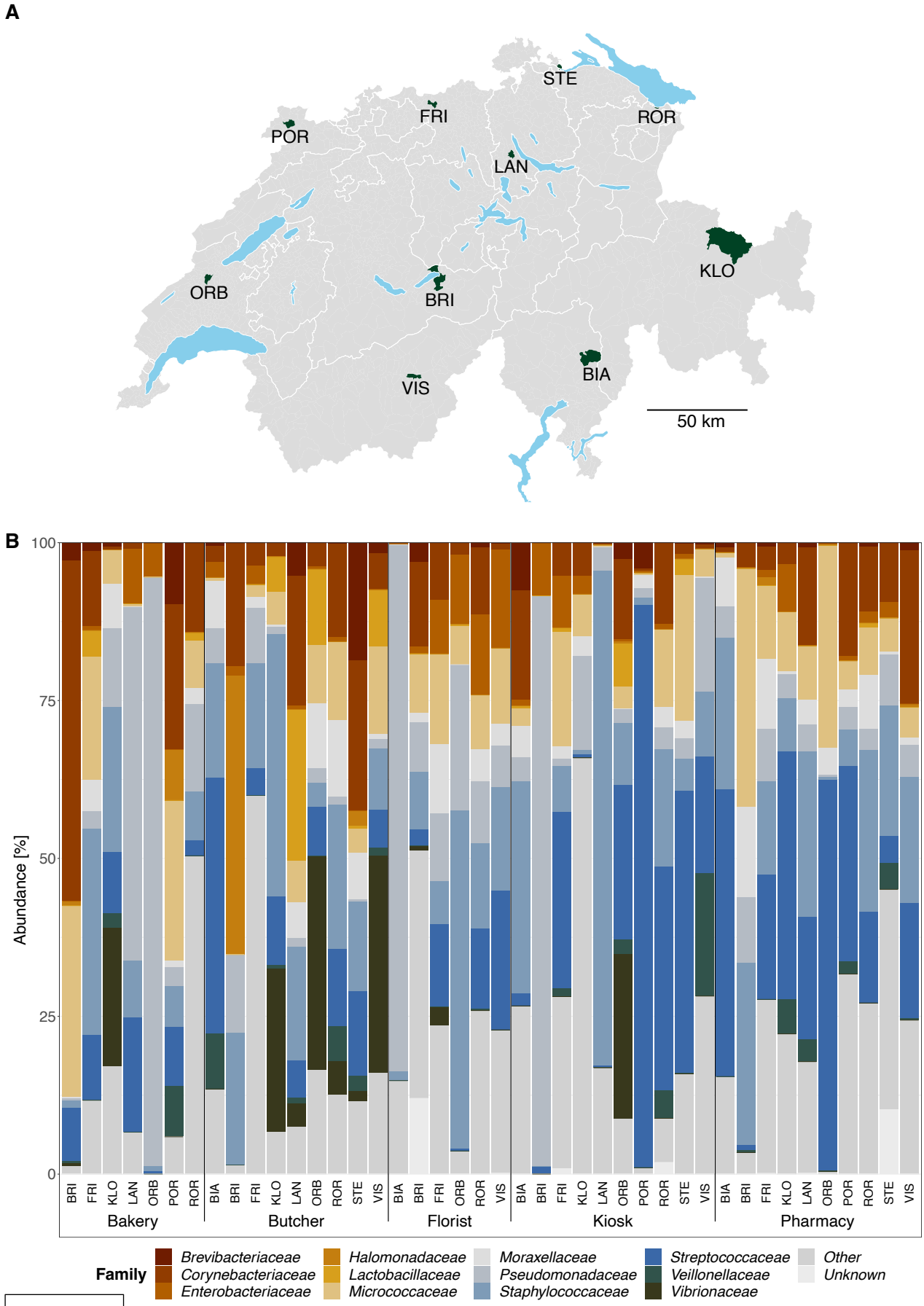

Figure 1.

Figure 1 (p. 25). Bacterial community composition across sampling locations and shop types. Panel A: Distribution of sampling locations across Switzerland. The map shows the 10 municipalities, highlighted in dark green, in which banknotes were collected. Panel B: Relative abundances of the main bacterial families identified by amplicon sequencing from banknotes sampled in each shop (lower *x*-axis) and location (upper *x*-axis, indicated by three-letter abbreviations). *Unknown* contains non-assigned ZOTUs; *Other* contains assigned ZOTUs not belonging to the most abundant families. Abbreviations in both panels: BIA = Biasca, BRI = Brienz BE, FRI = Frick, KLO = Klosters-Serneus, LAN = Langnau am Albis, ORB = Orbe, POR = Porrentruy, ROR = Rorschach, STE = Stein am Rhein, VIS = Visp.

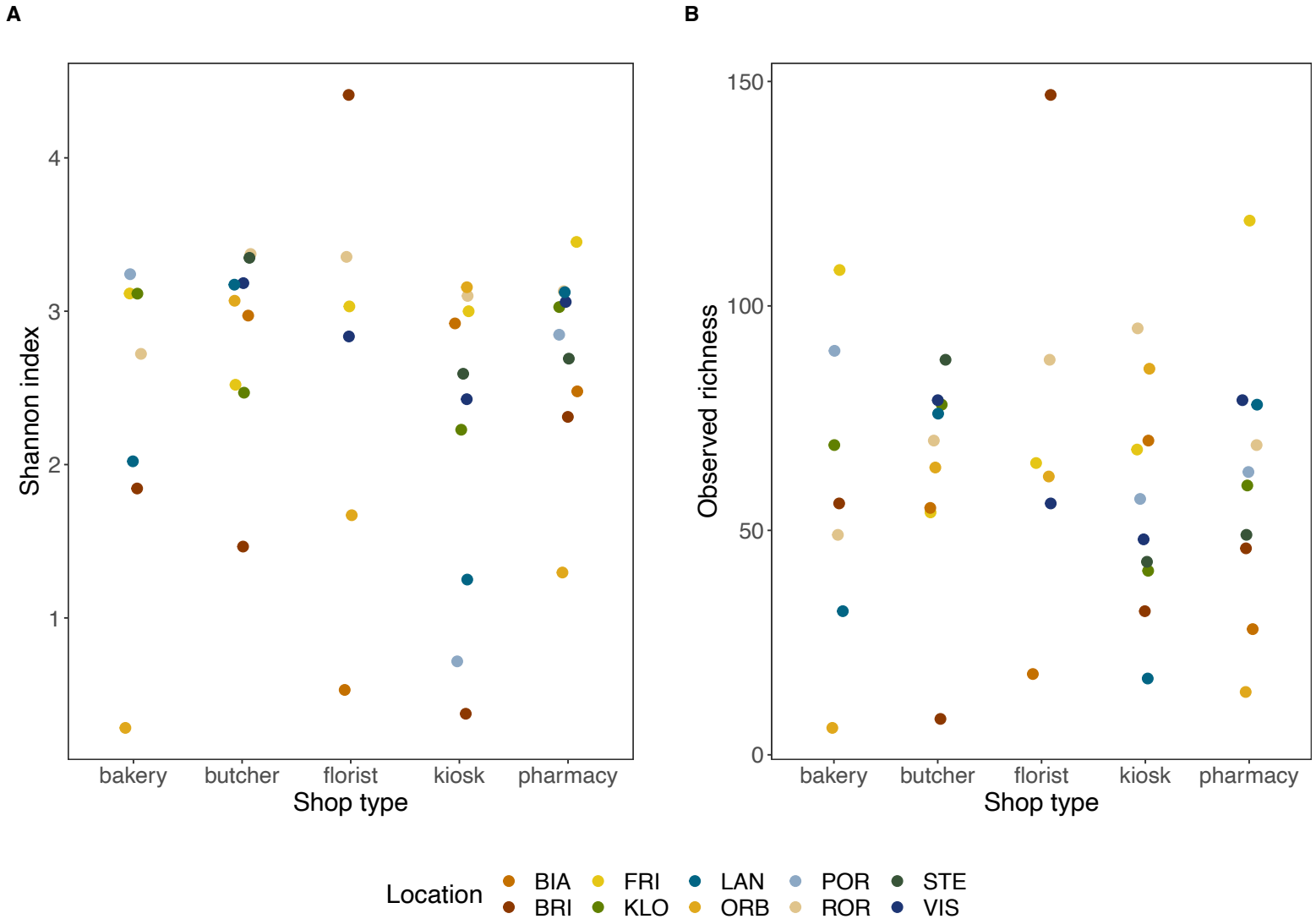

Figure 2. Within-sample taxonomic diversity of samples from banknotes collected in various shop types across Switzerland. Panel A: The Shannon diversity index *H* takes into account both richness (number of species present) and evenness (how evenly do present species occur). Panel B: Observed richness gives the number of unique ZOTUs present in a sample. Colours indicate locations (abbreviations: BIA = Biasca, BRI = Brienz BE, FRI = Frick, KLO = Klosters-Serneus, LAN = Langnau am Albis, ORB = Orbe, POR = Porrentruy, ROR = Rorschach, STE = Stein am Rhein, VIS = Visp). Values are jittered on the both axes in both panels.

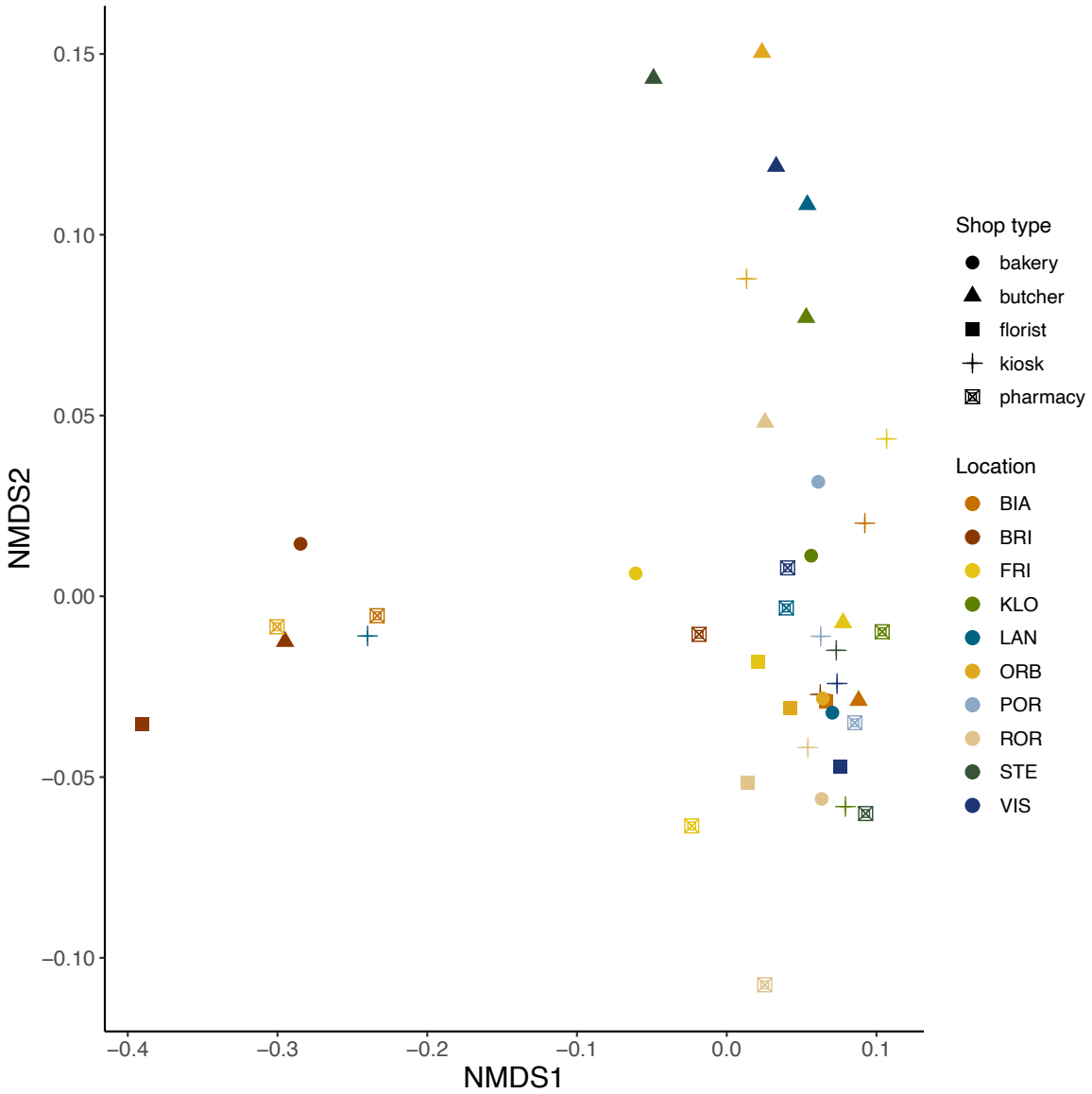

Figure 3. Ordination analysis. NMDS ordination based on Bray-Curtis dissimilarity between the bacterial communities isolated from banknotes (stress = 0.11). Symbols represent different shop types and are coloured according to location. Abbreviations: BIA = Biasca, BRI = Brienz BE, FRI = Frick, KLO = Klosters-Serneus, LAN = Langnau am Albis, ORB = Orbe, POR = Porrentruy, ROR = Rorschach, STE = Stein am Rhein, VIS = Visp.

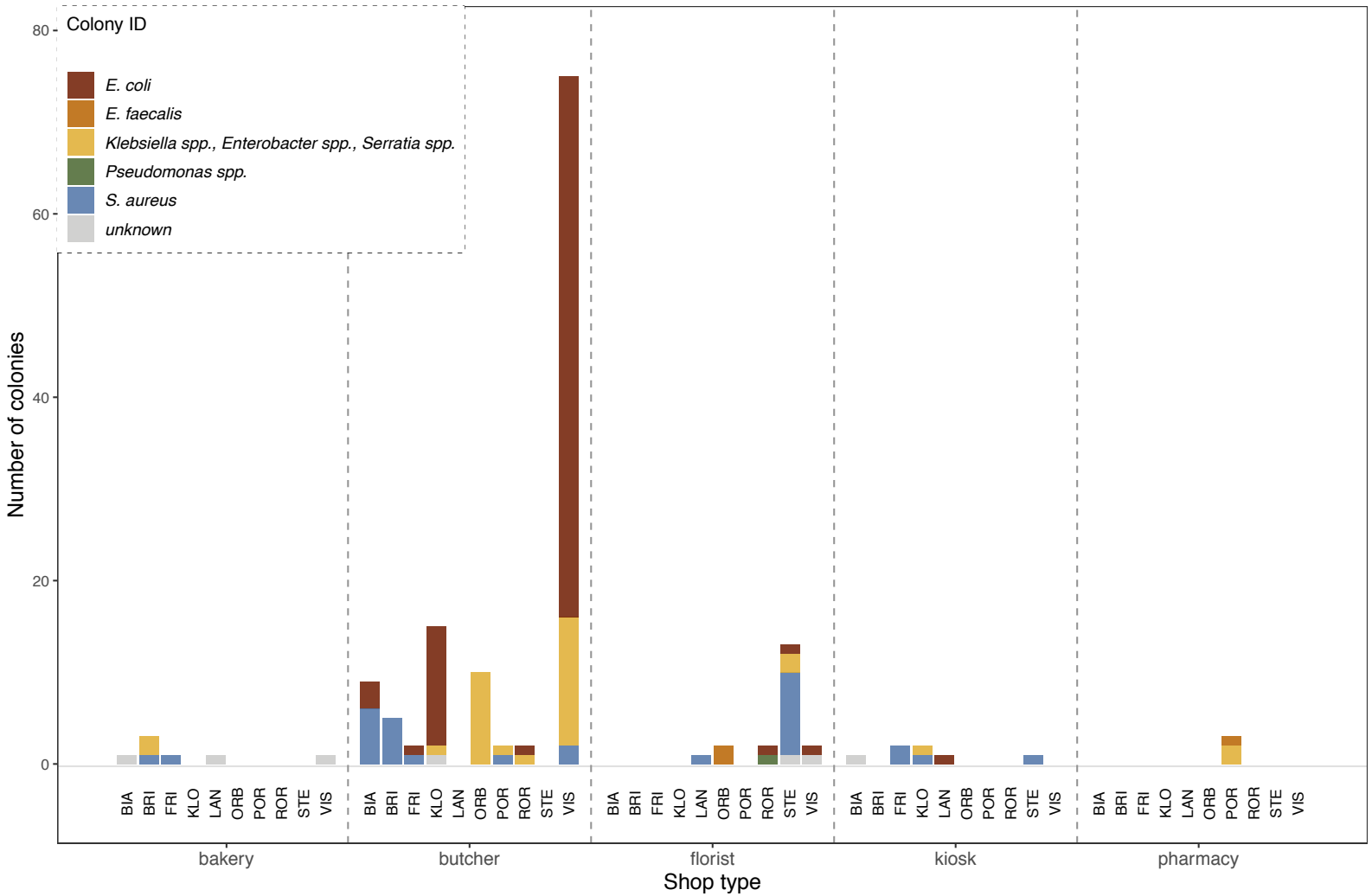

Figure 4. Number and identity of colonies isolated from banknotes collected in various shop types across Switzerland. Each composite bar gives the number and identity of colonies detected in samples isolated from banknotes. The bar colour indicates species identity (based on morphology and colour on Chromatic™ MH agar, see *Methods*). Colonies classified as "unknown" had uncertain identity (regular-shaped, small size) or a morphology more commonly associated with yeasts/fungi (astral appearance, polychromatic, with spores/fruiting body-like structures). Abbreviations: BIA = Biasca, BRI = Brienz BE, FRI = Frick, KLO = Klosters-Serneus, LAN = Langnau am Albis, ORB = Orbe, POR = Porrentruy, ROR = Rorschach, STE = Stein am Rhein, VIS = Visp.

Acknowledgments

AMB thanks Richard Allen, Elrina Bomben, Carole Imhof, Ricardo Leon Sampedro; Ethics Commission ETHZ, GDC ETHZ, Legal Services ETHZ, Statistical Consulting Group ETHZ. AMB and ARH thank Andrew Letten.

References

Allan, A., Cook, D., Gayler, R., Kirk, H., Peng, R., and Saber, E. (2021) ochRe: Australia-Themed Color Palettes.

Anderson, M.J. (2001) A new method for non-parametric multivariate analysis of variance. *Austral Ecol* **26**: 32–46.

De Angelis, M. and Gobbetti, M. (2011) Lactobacillus SPP.: General Characteristics. In *Encyclopedia of Dairy Sciences*. Fuquay, J.W. (ed). Academic Press; Copyright © 1999 Elsevier Ltd. All rights reserved., pp. 78–90.

De Angelis, M. and Gobbetti, M. (2016) Lactobacillus SPP.: General Characteristics ☆. *Ref Module Food Sci*.

Argandoña, M., Vargas, C., Reina-Bueno, M., Rodríguez-Moya, J., Salvador, M., and Nieto, J.J. (2012a) An extended suite of genetic tools for use in bacteria of the halomonadaceae: An overview. In *Methods in Molecular Biology*. Lorence, A. (ed). Heidelberg: Springer, pp. 167–201.

Argandoña, M., Vargas, C., Reina-Bueno, M., Rodríguez-Moya, J., Salvador, M., and Nieto, J.J. (2012b) An extended suite of genetic tools for use in bacteria of the halomonadaceae: An overview. *Methods Mol Biol* **824**: 167–201.

Baron, S., Ceccarelli, D., Dalsgaard, I., Granier, S.A., Haenen, O., Jansson, E., et al. (2020) Influence of incubation time on antimicrobial susceptibility testing of pathogenic Vibrio anguillarum and Vibrio vulnificus isolated from fish. *Aquaculture* **524**: 1–5.

Central Bank, E. (2020) Study on the payment attitudes of consumers in the euro area (SPACE).

Chao, A. (1984) Nonparametric estimation of the number of classes in a population. *Scand Sournal Stat* **11**: 265–270.

Chao, A. and Bunge, J. (2002) Estimating the number of species in a stochastic abundance model. *Biometrics* **58**: 531–539.

Chase, J.M. (2003a) Community assembly: When should history matter? *Oecologia* **136**: 489–498.

Chase, J.M. (2003b) Community assembly: when should history matter? *Oecologia* **136**: 489–498.

Chase, J.M. (2010) Stochastic community assembly causes higher biodiversity in more productive environments. *Science* **328**: 1388–1391.

Chase, J.M. and Myers, J.A. (2011) Disentangling the importance of ecological niches from stochastic processes across scales. *Philos Trans R Soc B Biol Sci* **366**: 2351–2363.

Chen, H. (2021) VennDiagram: Generate High-Resolution Venn and Euler Plots.

Chesson, P. (2000) Mechanisms of Maintenance of Species Diversity. *Annu Rev Ecol Syst* **31**: 343–66.

Clarke, K.R. (1993) Non-parametric multivariate analyses of changes in community structure. *Aust J Ecol* **18**: 117–143.

Clarke, K.R., Somerfield, P.J., and Chapman, M.G. (2006) On resemblance measures for ecological studies, including taxonomic dissimilarities and a zero-adjusted Bray-Curtis coefficient for denuded assemblages. *J Exp Mar Biol Ecol* **330**: 55–80.

Cocolin, L., Dolci, P., and Rantsiou, K. (2011) Biodiversity and dynamics of meat fermentations: The contribution of molecular methods for a better comprehension of a complex ecosystem. *Meat Sci* **89**: 296–302.

Cogen, A.L., Nizet, V., and Gallo, R.L. (2008) Skin microbiota: A source of disease or defence? *Br J Dermatol* **158**: 442–455.

Cousin, M.A. (1999) PSEUDOMONAS | Introduction. In *Encyclopedia of Food Microbiology*. Robinson, R.K.B.T.-E. of F.M. (ed). Oxford: Elsevier, pp. 1864–1867.

Cruaud, P., Vigneron, A., Dorea, C.C., Rodriguez, M.J., and Charette, S.J. (2020) Rapid Changes in Microbial Community Structures along a Meandering River. *Microorganisms* **8**: 1631.

Danko, D., Bezdan, D., Afshin, E.E., Ahsanuddin, S., Bhattacharya, C., Butler, D.J., et al. (2021) A global metagenomic map of urban microbiomes and antimicrobial resistance. *Cell* **184**: 3376–3393.

Dawson, W., Hör, J., Egert, M., van Kleunen, M., and Pester, M. (2017) A Small Number of Low-abundance Bacteria Dominate Plant Species-specific Responses during Rhizosphere Colonization. *Front Microbiol* **8**: 975.
Deibel, R.H., Wilson, G.D., and Niven, C.F. (1961) Microbiology of Meat Curing. *Appl Microbiol* **9**: 239–243.
Delanghe, L., Spacova, I., Van Malderen, J., Oerlemans, E., Claes, I., and Lebeer, S. (2021) The role of lactobacilli in inhibiting skin pathogens. *Biochem Soc Trans* **49**: 617–627.
Diamond, J.M. (1975) Assembly of species communities. *Ecol Evol Communities* 342–444.
Dourou, D., Spyrelli, E.D., Doulgeraki, A.I., Argyri, A.A., Grounta, A., Nychas, G.J.E., et al. (2021) Microbiota of chicken breast and thigh fillets stored under different refrigeration temperatures assessed by next-generation sequencing. *Foods* **10**: 1–17.
Ebach, M.C. (2015) Origins of Biogeography, Dordrecht: Springer Netherlands.
Edgar, R.C. (2010) Search and clustering orders of magnitude faster than BLAST. *Bioinformatics* **26**: 2460–2461.
Edgar, R.C. (2016a) SINTAX: a simple non-Bayesian taxonomy classifier for 16S and ITS sequences, Bioinformatics.
Edgar, R.C. (2016b) UNOISE2: improved error-correction for Illumina 16S and ITS amplicon sequencing, Bioinformatics.
Fargione, J., Brown, C.S., and Tilman, D. (2003) Community assembly and invasion: An experimental test of neutral versus niche processes. *Proc Natl Acad Sci U S A* **100**: 8916–8920.
Federal Office of Statistics (2020) Erwerbstätige nach Wohn- und Arbeitsgemeinde, 2018 (CSV-Datei).
Felis, G.E. and Pot, B. (2014) The family Lactobacillaceae. In *Lactic Acid Bacteria: Biodiversity and Taxonomy*. Holzapfel, W.H. and Wood, B.J. (eds). John Wiley & Sons, Ltd., pp. 245–247.
Fierer, N. (2017) Embracing the unknown: Disentangling the complexities of the soil microbiome. *Nat Rev Microbiol* **15**: 579–590.
Fierer, N., Hamady, M., Lauber, C.L., and Knight, R. (2008) The influence of sex, handedness, and washing on the diversity of hand surface bacteria.
Finlay, B.J. (2002) Global dispersal of free-living microbial eukaryote species. *Science* **296**: 1061–1063.
da Fonseca, T.A.P., Pessôa, R., and Sanabani, S.S. (2015) Molecular analysis of bacterial microbiota on Brazilian currency note surfaces. *Int J Environ Res Public Health* **12**: 13276–13288.
Forquin, M.P. and Weimer, B.C. (2014) Brevibacterium. *Encycl Food Microbiol Second Ed* **1**: 324–330.
Fourquin-Gomez, M.-P., Weimer, B.C., Sorieul, L., Kalinowski, J., and Vallaeys, T. (2014) The Family Brevibacteriaceae. In *The Prokaryotes: Actinobacteria*. Rosenberg, E., DeLong, E.F., Lory, S., Stackebrandt, E., and Thompson, F. (eds). Heidelberg: Springer, pp. 141–153.
Franz, C.M.A.P., Endo, A., Abriouel, H., Van Reenen, C.A., Gálvez, A., and Dicks, L.M.T. (2014) The genus Pediococcus.
Fuertes-Perez, S., Hauschild, P., Hilgarth, M., and Vogel, R.F. (2019) Biodiversity of Photobacterium spp. Isolated From Meats. *Front Microbiol* **10**:.
Galili, T. (2015) dendextend: an R package for visualizing, adjusting and comparing trees of hierarchical clustering. *Bioinformatics* **31**: 3718–3720.
Gehring, B., Graf, S., and Trütsch, T. Swiss Payment Monitor 2020 Wie bezahlt die Schweiz?
Guo, K. and Gao, P. (2021) microbial: Do 16s Data Analysis and Generate Figures.
Hanson, C.A., Fuhrman, J.A., Horner-Devine, M.C., and Martiny, J.B.H. (2012) Beyond biogeographic patterns: Processes shaping the microbial landscape. *Nat Rev Microbiol* **10**: 497–506.
Heshiki, Y., Dissanayake, T., Zheng, T., Kang, K., Yueqiong, N., Xu, Z., et al. (2017) Toward a metagenomic understanding on the bacterial composition and resistome in Hong Kong banknotes. *Front Microbiol* **8**:.
Hillebrand, H., Watermann, F., Karez, R., and Berninger, U.G. (2001) Differences in species richness patterns between unicellular and multicellular organisms. *Oecologia* **126**: 114–124.
HilleRisLambers, J., Adler, P.B., Harpole, W.S., Levine, J.M., and Mayfield, M.M. (2012) Rethinking community assembly through the lens of coexistence theory. *Annu Rev Ecol Evol Syst* **43**: 227–248.
Horner-Devine, M.C., Lage, M., Hughes, J.B., and Bohannan, B.J.M. (2004) A taxa-area relationship for bacteria. *Nature* **432**: 750–753.
Hubbell, S.P. (2011) The Unified Neutral Theory of Biodiversity and Biogeography (MPB-32), Princeton University Press.
Huber, W., von Heydebreck, A., Sultmann, H., Poustka, A., and Vingron, M. (2002) Variance stabilization applied to microarray data calibration and to the quantification of differential expression. *Bioinformatics* **18**: S96–S104.
Jackman, S. (2020) pscl: Classes and Methods for R., Sydney, New South Wales, Australia.: Developed in the Political Science Computational Laboratory (United States Studies Centre, University of Sydney).

Jalali, S., Kohli, S., Latka, C., Bhatia, S., Vellarikal, S.K., Sivasubbu, S., et al. (2015) Screening currency notes for microbial pathogens and antibiotic resistance genes using a shotgun metagenomic approach. *PLoS ONE* **10**:.

Kandlikar, G. (2021) ranacapa: Utility Functions and "shiny" App for Simple Environmental DNA Visualizations and Analyses.

Kassambara, I. (2020) ggpubr: 'ggplot2'-Based Publication Ready Plots.

Kim, K.K., Lee, J.S., and Stevens, D.A. (2013) Microbiology and epidemiology of Halomonas species. *Future Microbiol* **8**: 1559–1573.

Kraenzlin, S., Meyer, C., and Nellen, T. (2020) COVID-19 and regional shifts in Swiss retail payments (Version of July 23, 2020).

Lahti, L. and Shetty, S. (2012) microbiome R package.

Lahti, L., Shetty, S., and et al. (2017) Tools for microbiome analysis in R.

Leisner, J.J. and Pot, B. (2014) The genus Paralactobacillus.

Libertucci, J. and Young, V.B. (2019) The role of the microbiota in infectious diseases. *Nat Microbiol* **4**: 35–45.

Lin, J., Jiang, W., Shi, Y., and Cai, W. (2021) Metagenomic Sequencing Revealed the Potential Pathogenic Threats of Banknotes. *ACS Omega* **6**: 3499–3507.

Lonvaud-Funel, A. (2014) Leuconostocaceae Family, Second Edi. Elsevier.

Love, M.I., Huber, W., and Anders, S. (2014) Moderated estimation of fold change and dispersion for RNA-seq data with DESeq2. *Genome Biol* **15**: 550.

Macarthur, R. and Levins, R. (1967) The Limiting Similarity, Convergence, and Divergence of Coexisting Species. *Am Nat* **101**: 377–385.

Madhaiyan, M., Wirth, J.S., and Saravanan, V.S. (2020) Phylogenomic analyses of the Staphylococcaceae family suggest the reclassification of five species within the genus Staphylococcus as heterotypic synonyms, the promotion of five subspecies to novel species, the taxonomic reassignment of five Staphylococcu. *Int J Syst Evol Microbiol* **70**: 5926–5936.

Mahendra, M. (2019) phyloseq-extended: R package.

Maritz, J.M., Sullivan, S.A., Prill, R.J., Aksoy, E., Scheid, P., and Carlton, J.M. (2017) Filthy lucre: A metagenomic pilot study of microbes found on circulating currency in New York City. *PLoS ONE* **12**: e0175527.

McMurdie, P.J. and Holmes, S. (2013) phyloseq: An R Package for Reproducible Interactive Analysis and Graphics of Microbiome Census Data. *PLoS ONE* **8**: e61217.

Murphy, T.F. and Parameswaran, G.I. (2009) Moraxella catarrhalis, a human respiratory tract pathogen. *Clin Infect Dis* **49**: 124–131.

Nieminen, T.T., Dalgaard, P., and Björkroth, J. (2016) Volatile organic compounds and Photobacterium phosphoreum associated with spoilage of modified-atmosphere-packaged raw pork. *Int J Food Microbiol* **218**: 86–95.

Oksanen, J., Blanchet, G., Friendly, M., Kindt, R., Legendre, P., McGlinn, D., et al. (2020) vegan: Community Ecology Package.

Oren, A. (2011) The Halophilic World of Lourens Baas Becking. In *Halophiles and Hypersaline Environments*. Ventosa, A., Oren, A., and Ma, Y. (eds). Heidelberg: Springer, pp. 9–25.

Padgham, M. and Sumner, M. (2021) geodist: Fast, Dependency-Free Geodesic Distance Calculations.

Paradis, E. and Schliep, K. (2019) ape 5.0: an environment for modern phylogenetics and evolutionary analyses in R. *Bioinformatics* **35**: 526–528.

Pennacchia, C., Ercolini, D., and Villani, F. (2011) Spoilage-related microbiota associated with chilled beef stored in air or vacuum pack. *Food Microbiol* **28**: 84–93.

Phillips, N. (2017) yarrr: A Companion to the e-Book "YaRrr!: The Pirate's Guide to R".

Połka, J., Rebecchi, A., Pisacane, V., Morelli, L., and Puglisi, E. (2015) Bacterial diversity in typical Italian salami at different ripening stages as revealed by high-throughput sequencing of 16S rRNA amplicons. *Food Microbiol* **46**: 342–356.

Pot, B., Felis, G.E., De Bruyne, K., Tsakalidou, E., Papadimitriou, K., Leisner, J., and Vandamme, P. (2014) The genus Lactobacillus.

R Core Team (2021) R: A language and environment for statistical computing., Vienna, Austria: R Foundation for Statistical Computing.

Rajaram, S. and Oono, Y. (2010) NeatMap - non-clustering heat map alternatives in R. *BMC Bioinformatics* **11**: 45.

Reese, A.T., Madden, A.A., Joossens, M., Lacaze, G., and Dunn, R.R. (2020) Influences of Ingredients and Bakers on the Bacteria and Fungi in Sourdough Starters and Bread. *mSphere* **5**: 1–15.

Robert-Pillot, A., Copin, S., Himber, C., Gay, M., and Quilici, M.L. (2014) Occurrence of the three major Vibrio species pathogenic for human in seafood products consumed in France using real-time PCR. *Int J Food Microbiol* **189**: 75–81.

Rock, C. and Donnenberg, M.S. (2014) Human Pathogenic Enterobacteriaceae. In *Reference Module in Biomedical Sciences*. Elsevier.
Salonen, A., Salojärvi, J., Lahti, L., and de Vos, W.M. (2012) The adult intestinal core microbiota is determined by analysis depth and health status. *Clin Microbiol Infect* **18**: 16–20.
Samelis, J., Maurogenakis, F., and Metaxopoulos, J. (1994) Characterisation of lactic acid bacteria isolated from naturally fermented Greek dry salami. *Int J Food Microbiol* **23**: 179–196.
Schaarschmidt, J. (1884) Upon the occurrence of bacteria and minute algæ on the surface of paper money [3]. *Nature* **30**: 360.
Schmieder, R. and Edwards, R. (2011) Quality control and preprocessing of metagenomic datasets. *Bioinforma Oxf Engl* **27**: 863–864.
Shade, A. and Handelsman, J. (2012) Beyond the Venn diagram: The hunt for a core microbiome. *Environ Microbiol* **14**: 4–12.
Sierra, M.L., Gonzalez-Fandos, E., García-López, M.L., Camino Garcia Fernandez, M., and Prieto, M. (1995) Prevalence of salmonella, yersinia, aeromonas, campylobacter, and cold-growing escherichia coli on freshly dressed lamb carcasses. *J Food Prot* **58**: 1183–1185.
Skowron, K., Bauza-Kaszewska, J., Kraszewska, Z., Wiktorczyk-Kapischke, N., Grudlewska-Buda, K., Kwiecińska-Piróg, J., et al. (2021) Human skin microbiome: Impact of intrinsic and extrinsic factors on skin microbiota. *Microorganisms* **9**: 543.
Smith, S. (2021) phylosmith: Functions to help analyze data as phyloseq objects.
Stegen, J.C., Lin, X., Fredrickson, J.K., and Konopka, A.E. (2015) Estimating and mapping ecological processes influencing microbial community assembly. *Front Microbiol* **6**:.
Takemura, A.F., Chien, D.M., and Polz, M.F. (2014) Associations and dynamics of vibrionaceae in the environment, from the genus to the population level. *Front Microbiol* **5**:.
Tauch, A. and Sandbote, J. (2014) The Family Corynebacteriaceae. In *The Prokaryotes: Actinobacteria*. Rosenberg, E., Delong, E.F., Lory, S., Stackebrandt, E., and Thompson, F. (eds). Heidelberg: Springer, pp. 239–278.
Thomas, Y., Vogel, G., Wunderli, W., Suter, P., Witschi, M., Koch, D., et al. (2008) Survival of influenza virus on banknotes. *Appl Environ Microbiol* **74**: 3002–3007.
Vinet, L. and Zhedanov, A. (2011) A "missing" family of classical orthogonal polynomials. In *Journal of Physics A: Mathematical and Theoretical*. Rosenbert, E., DeLong, E.F., Lory, S., Stackebrandt, E., and Thompson, F. (eds). Heidelberg: Springer, pp. 443–476.
Vriesekoop, F., Chen, J., Oldaker, J., Besnard, F., Smith, R., Leversha, W., et al. (2016) Dirty money: A matter of bacterial survival, adherence, and toxicity. *Microorganisms* **4**:.
Walter, J. (2008) Ecological role of Lactobacilli in the gastrointestinal tract: Implications for fundamental and biomedical research. *Appl Environ Microbiol* **74**: 4985–4996.
Wareing, P. (2016) Microbiology of soft drinks and fruit juices. In *Chemistry and Technology of Soft Drinks and Fruit Juices*. Ashurst, P.R. (ed). Chichester: John Wiley & Sons, Ltd., pp. 290–309.
Webb, C.O. Exploring the Phylogenetic Structure of Ecological Communities: An Example for Rain Forest Trees.
Weiss, S., Xu, Z.Z., Peddada, S., Amir, A., Bittinger, K., Gonzalez, A., et al. (2017) Normalization and microbial differential abundance strategies depend upon data characteristics. *Microbiome* **5**: 1–18.
Whitaker, R.J., Grogan, D.W., and Taylor, J.W. (2003a) Geographic barriers isolate endemic populations of hyperthermophilic archaea. *Science* **301**: 976–978.
Whitaker, R.J., Grogan, D.W., and Taylor, J.W. (2003b) Geographic barriers isolate endemic populations of hyperthermophilic archaea. *Science* **301**: 976–978.
Wickham, H. (2009) ggplot2: elegant graphics for data analysis, New York: Springer.
Wickham, H., François, R., Henry, L., and Müller, K (2021) dplyr: A Grammar of Data Manipulation.
Wilke, C. (2020) cowplot: Streamlined Plot Theme and Plot Annotations for "ggplot2".
Zapala, M.A. and Schork, N.J. (2006) Multivariate regression analysis of distance matrices for testing associations between gene expression patterns and related variables. *Proc Natl Acad Sci U S A* **103**: 19430–19435.
Zhou, J., Kang, S., Schadt, C.W., and Garten, C.T. (2008) Spatial scaling of functional gene diversity across various microbial taxa. *Proc Natl Acad Sci U S A* **105**: 7768–7773.
Zhou, J., Liu, W., Deng, Y., Jiang, Y.H., Xue, K., He, Z., et al. (2013) Stochastic assembly leads to alternative communities with distinct functions in a bioreactor microbial community. *mBio* **4**:.
Zhou, J. and Ning, D. (2017) Stochastic Community Assembly: Does It Matter in Microbial Ecology?
Zumbach, D. (2019) RSwissMaps: Plot and Save Customised Swiss Maps.

883 **Data Accessibility and Benefit-Sharing Statement**

884 The sequencing data have been deposited in the European Nucleotide Archive under the study
885 accession number PRJEB45390 (https://www.ebi.ac.uk/ena; data will be made accessible upon
886 publication of the study).

887 Other data presented in this study will be made available at the Dryad Digital Repository:
888 http://dx.doi.org/...: to be completed after manuscript is accepted for publication.

889 Benefits Generated: Benefits from this research accrue from the sharing of our data and
890 results on public databases as described above.

891
892 **Author Contributions**

893 AMB, ARH	designed research.
894 AMB	performed research.
895 AMB, ARH	analyzed data.
896 AMB, ARH	wrote paper.